ATOMIC AND MOLECULAR PHYSICS USING POSITRON TRAPS AND TRAP-BASED BEAMS

C. M. Surko

Physics Department, University of California, San Diego, La Jolla, CA 92093-0319
csurko@ucsd.edu

Abstract: Techniques to accumulate and cool positrons in Penning traps provide new tools to study atomic and molecular physics and chemistry. This chapter presents an overview of studies of the interaction of low-energy positrons with atoms and molecules using these methods. In the vacuum environment of a trap, isolated two-body interactions of positrons with atoms and molecules can be studied with precision. Measurements include annihilation rates, Z_{eff}, as a function of both atomic and molecular species and positron temperature. Doppler-broadening studies provide information about the electronic states involved in the annihilation process. Positron accumulation techniques have also enabled the creation of cold, bright low-energy positron beams. High-resolution scattering measurements are described, including absolute measurements of the cross sections for vibrational excitation of molecules. Prospects for future developments in these areas are also discussed.

1.   OVERVIEW

Positron-matter interactions are important in areas of atomic physics, condensed matter physics and gamma-ray astronomy, and for technological applications including mass spectroscopy and characterization of solid surfaces [1-4]. Study of the interaction of positrons with atoms and molecules has a long history [1, 5-11]. Many aspects of these interactions are understood, such as scattering processes at energies above a few electron Volts. Nevertheless, important phenomena remain to be studied, particularly those that require high-

resolution positron sources and those occurring at smaller values of positron energy. One problem of current interest is understanding positron annihilation in large molecules [12-16]. Another example is the excitation of molecular vibrations by positron impact [17-19]. Low-energy processes such as these are important in establishing a predictive antimatter-matter chemistry, a field that is likely to blossom in the next few years as low energy antimatter becomes more readily available in the laboratory [20-26].

Historically, progress in positron research has been limited by the availability of high-flux positron sources and bright positron beams. This has been a particular hindrance in studying low-energy positron interactions. The development of efficient positron accumulators has changed this situation [24, 27, 28], and this chapter summarizes experimental measurements enabled by positron traps and trap-based beams. The work focuses on two physical processes involving atoms and molecules -- positron scattering and annihilation at low energies (e.g., positron energies below the threshold for positronium formation).

There have been extensive studies of positron annihilation on atoms and molecules in work spanning several decades [5, 8, 9]. Typically these experiments were conducted by injecting fast positrons into gases at pressures ~ 1 atmosphere. Annihilation was measured as the positrons thermalize to the ambient gas temperature (~ 300 K). Many important results were established, including quantitative measures of the normalized annihilation rate, Z_{eff} at the ambient temperature, and the fact that Z_{eff} depends on chemical species and can increase by orders of magnitude for modest changes in molecular size.

The development of Penning traps to accumulate positrons provided new opportunities to study positron annihilation [12-15]. The positrons are in ultra-high vacuum in the presence of a very low-pressure test gas, and this provides the opportunity to study the isolated, two-body interaction of positrons with atoms or molecules. In this environment there is no question about the thermalization of the positrons or the possibility of multiple-molecule correlations or clustering. Molecules with low vapor pressures can be studied conveniently. The positrons can be confined for long times in the accumulator in order to maximize the interaction with the test species. This is particularly useful for studying weak processes where the signal-to-noise ratio is an important consideration. Using this method, annihilation studies have now been conducted for a wide range of atoms and molecules, resulting in comprehensive data for positron annihilation as a function of chemical species and extending by orders of magnitude the maximum experimentally measured values of Z_{eff}. The trapped positrons can also be heated by the application of radio frequency noise applied to the confining electrodes to study the dependence of Z_{eff} on positron temperature [15, 29].

Microscopic information about the annihilation process can be obtained by studying the Doppler-broadening of the 511-keV annihilation gamma-ray line [30, 31]. These measurements yield the momentum distributions of the annihilating electron-positron pairs which, for positrons with energies ≤ 1 eV, is dominated by the momentum distribution of the bound electrons. This technique has been used

to identify the annihilation sites (i.e., the specific electronic states) in atoms and molecules.

A short summary of the state of the positron annihilation studies is that, in cases where measurements and predictions can be compared, measurements in atoms are generally in fair to good quantitative agreement with theoretical predictions. In contrast, the experiments in molecules raise a number of important theoretical questions, such as the physical mechanisms responsible for high annihilation rates. Many of these issues are now beginning to be addressed.

The availability of efficient positron accumulators led to the development of a new method to create cold, bright low-energy positron beams [32, 33]. With energy resolution ≤ 20 meV and tunable over energies from < 100 meV to many electron Volts, these beams have enabled a new generation of scattering experiments [18, 19]. Although the potential of this technique has yet to be fully exploited, it offers the possibility of providing absolute measurements of total and differential cross sections down to energies ≤ 100 meV. In this chapter, examples of recent work are described, including the first studies of the excitation of molecular vibrations by positrons. Comparisons between theory and experiment have been insightful (particularly in the case of vibrational excitation), and they raise a number of new and interesting questions that warrant further study.

After reviewing the current state of positron annihilation and scattering studies, this chapter concludes with a look to the future, describing possible extensions of a number of facets of the research. Work related to the topics discussed in this chapter can be found elsewhere in this volume. This includes theoretical discussions of positron-molecule interactions (Gianturco, *et al.*, Gribakin, Tachikawa, *et al.*, and Varella, *et al.*), extensions of the scattering studies described here and their relation to analogous electron experiments (Buckman), further development of new techniques to create trap-based positron beams (Greaves), and other studies with low-energy positrons involving positron accumulators (Charlton).

2. BUFFER-GAS ACCUMULATOR OPERATION

The principle of operation of the buffer-gas positron accumulator is described in detail elsewhere [24, 27, 28, 34]. Positrons from a radioactive ^{22}Na source are slowed to a few electron Volts using a neon rare-gas moderator. They are then injected into a series of cylindrical electrodes in the presence of a low-pressure N_2 buffer gas in an applied axial magnetic field ~ 0.15 T. The electrodes and differential pumping create three stages, each with successively lower N_2 gas pressure and electrostatic potential. Following a series of inelastic collisions with the N_2 molecules, the positrons are trapped in the third stage where the pressure is $\sim 1.5 \times 10^{-6}$ torr. The positrons cool to 300 K (i.e., room temperature) in ~ 1 s. More rapid cooling ($\tau \leq 0.1$ s) is obtained by adding $\sim 5 \times 10^{-7}$ torr of CF_4 or SF_6

to the third stage of the trap [35, 36]. The lifetime in the third stage is $\geq$ 40 s, limited by annihilation on the N_2. The buffer-gas trapping can be very efficient, with ~ 25% of slow positrons from the moderator trapped and cooled. Using this technique and a 90 mCi ^{22}Na source, plasmas containing ~ 3 x 10^8 positrons have been accumulated in a few minutes. The buffer gas can be pumped out in a few seconds, resulting in a positron lifetime ranging from tens of minutes to hours depending upon the quality of the vacuum. The number of positrons in the trap is measured by measuring the charge or annihilation gamma rays produced when the plasma is dumped on a collector plate. The temperature of the trapped positrons is measured routinely by measuring the tail of the energy distribution of positrons escaping from the trap.

3.   ANNIHILATION ON ATOMS AND MOLECULES

The annihilation rate is a sensitive measure of short-range correlations between the positron and the bound electrons. We follow the convention of expressing the annihilation rate Γ in terms of the parameter Z_{eff}, which is the annihilation rate relative to that for positrons in a gas of uncorrelated electrons (i.e., the Dirac annihilation rate).
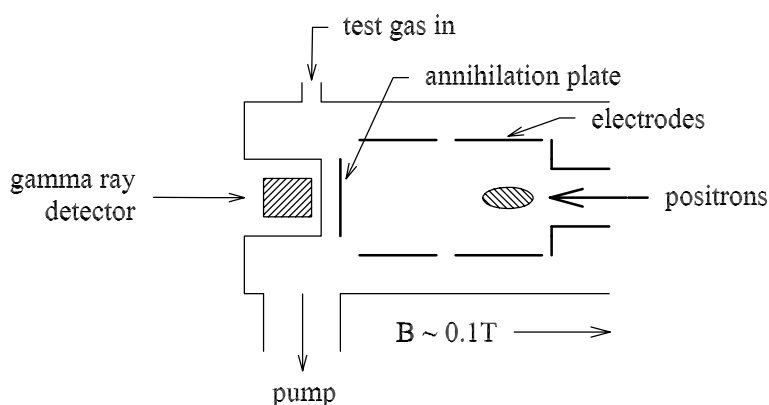
$$\Gamma = \pi r_0{}^2 c n_m Z_{eff},$$ (1)

where r_0 is the classical electron radius, c is the speed of light, and n_m is the number density of atoms or molecules. For large molecules, it is well established that Z_{eff} can greatly exceed the total number of electrons Z in the molecule [5, 8, 12-14]. Consequently, Z_{eff} *should be viewed as a normalized annihilation rate -- it bears no relation to the charge on the nucleus or the number of electrons in the molecule.* While the physical process responsible for these high annihilation rates is not fully understood, these large rates have been viewed as evidence for the existence of (long-lived) positron-molecule complexes [5, 6, 12, 13, 16].

The experimental arrangement for positron annihilation studies in the positron accumulator is shown in Fig. 1 [12-15]. Annihilation rates are measured after the positrons are trapped and cooled to room temperature by measuring the number of positrons, N_p, remaining as a function of time in the presence of a test gas. Typically the number of positrons remaining is measured by dumping the positron plasma on a metal plate and measuring the annihilation gamma rays. The rate is then given by $\Gamma = d[ln(N_p)]/dt$, where t is time. These experiments can be done either in the presence or absence of the N_2 buffer gas used for positron trapping. In order to reduce the density of impurity molecules in the system (base pressure $\leq$ 1 x 10^{-9} torr), a cryosurface was placed *in situ* in the vacuum chamber as necessary. It was cooled with either liquid nitrogen (to 77K) or with an ethanol-water mixture (to ~ 266 K), depending on the atomic or molecular species studied. The measured annihilation rates are found to be a

linear function of the test gas pressure (i.e., proportional to n_m), and the slope yields Z_{eff}. The linearity of the slope provides evidence that annihilation is due to isolated two-body interactions between the positrons and the test molecule.

Shown in Fig. 2 are data for a wide range of chemical species [12-15]. Note the very large differences in rates observed for only modest changes in chemical structure. Values of $Z_{eff} \sim 10^4$ had been measured previously in the high-pressure experiments [5, 6, 8]. The development of the positron trap enabled the extension of these studies to even larger molecular species including those that are liquids and solids at room temperature. The extremely broad range of

Figure 1. Schematic diagram of the apparatus used to study positron annihilation. The positrons are confined in a Penning trap by potentials applied to the electrodes and a magnetic field, B. Annihilation rates are measured by storing the positrons for various times in the presence of a test gas, then measuring the number of positrons remaining by dumping them on a plate and measuring the gamma ray signal. The Doppler linewidth of the gamma rays is measured using a Ge detector placed in close proximity to the trapped positrons.

observed values of Z_{eff} provides evidence of *qualitative* changes in the nature of the positron molecule interaction for relatively modest changes in chemical species. While the smaller values (e.g., $Z_{eff} \sim Z$) can be explained in terms of a simple collision model, larger values appear to require a different physical picture, such as the formation of positron-molecule resonances. Murphy *et al.*, pointed out that Z_{eff} for atoms and single-bonded molecules obeys a universal scaling as a function of $(E_i - E_{Ps})^{-1}$, which is shown in Fig. 3 [13]. To date, there has been no satisfactory explanation of this empirical relationship, beyond the speculation that large annihilation rates might be thought of in terms of positron-molecule complexes in which a positronium atom is attached to the corresponding positive ion [13].

The microscopic nature of positron interactions with atoms and molecules can be studied by measuring the Doppler-broadening of the 511-keV annihilation gamma-ray line [30, 31]. The Doppler linewidth is determined by the momentum
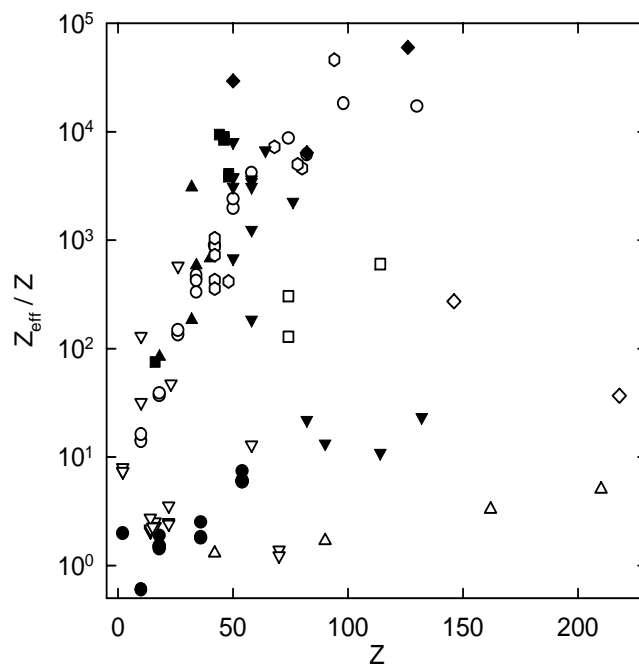
Figure 2. (a) Experimental values of Z_{eff}/Z plotted against Z, illustrating the fact that this quantity varies by orders of magnitude for modest changes in chemical species: (•) noble gases, (∇) simple molecules, (O) alkanes, (Δ) perfluorinated alkanes, ($\square$) perchlorinated alkanes, ($\Diamond$) perbrominated and periodated alkanes, (■) alkenes, (▲) oxygen-containing hydrocarbons, (O) ring hydrocarbons, (▼) substituted benzenes, and (♦) large organic molecules.

distribution of the electrons (i.e., determined by the electron quantum states) participating in the annihilation process. Shown in Fig. 4 is the gamma ray spectrum for positron annihilation on helium atoms. Also shown is a theoretical calculation by Van Reeth and Humberston [37]. Theory and experiment are in excellent agreement for the shape of the linewidth. There is also good agreement between theory and experiment for the annihilation linewidths of other noble gases [31]. These comparisons were made for annihilation on valence electrons. A careful search was also made in noble gas atoms for evidence of inner-shell annihilation, which would produce a broad, low-amplitude wing on the annihilation line. Annihilation was observed on the next inner shell, but only at the few percent level, and then only in larger atoms, Kr (1.3 %) and Xe (2.4 %) [31]. The fact that these percentages are low is consistent with the highly repulsive (core) potential that the positron experiences once it begins to penetrate the valence electrons.

The gamma-ray linewidth provides relatively direct information about the specific electronic states participating in the annihilation process. A systematic study was done in alkane molecules in which the linewidth was measured as a function of the fraction of C - C and C - H bonds in the molecule, and the results
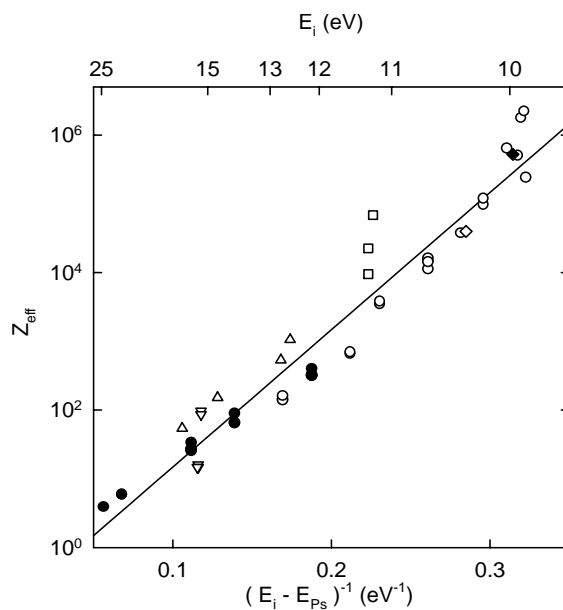
6

Figure 3. Values of Z_{eff} for noble gas atoms and single-bonded molecules as a function of $(E_i - E_{Ps})^1$, where E_i is the ionization energy and E_{Ps} is the positronium formation energy. (See Ref. [14] for details.)
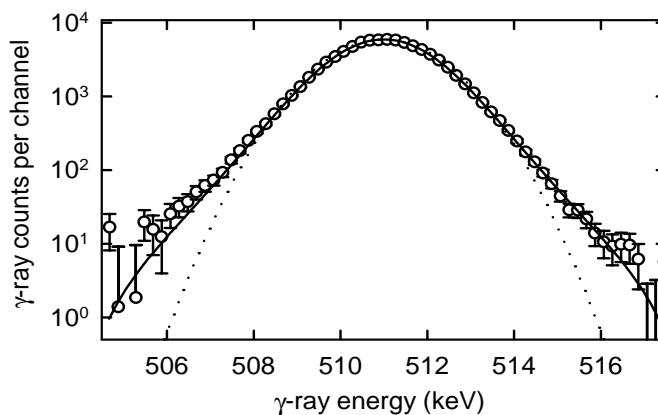

Figure 4. Annihilation gamma-ray spectrum from He: (O) experiment, (−) theoretical calculation including detector response, and (···) a Gaussian fit. (From Ref. [37])

are shown in Fig. 5 (a) [15]. When compared with calculations for the linewidths of the C-C and C-H bonds [38], these data are consistent with annihilation occurring with roughly equal probability on any of the valence electrons. This is only an approximate statement; and since the calculations of Ref. [38] are now more than three decades old, further theoretical study of the momentum distribution expected for electrons in valence orbitals in hydrocarbons would be

helpful. A similar study of Doppler linewidths was done in hydrocarbons in which the H atoms were systematically substituted with fluorines [15]. In this case, the measured linewidths can be accurately fit by a linear combination of the linewidths measured for pure fluorocarbons and pure hydrocarbons. The results of this analysis are shown in Fig. 5 (b). This analysis also implies that annihilation occurs with approximately equal probability on any valence electron, which in this case includes the valence electrons in the fluorine atoms in addition to those in the C - H and C - C bonds.

In summary, all results to date are consistent with most of the annihilation occurring on any of the valence electrons (as opposed to favoring specific sites in the molecule) with a small fraction of the annihilation occurring on the next inner shell when heavier atoms are present. This can be interpreted to mean that the positron has a relatively long de Broglie wavelength in the vicinity of the molecule. Consequently, the positron interacts with roughly equal probability with any of the valence electrons. This picture is in contrast to the case where the positron is localized at a specific molecular site, as would be expected in a tight-binding model. The lack of preference for annihilation on specific valence electrons is consistent with the model developed by Crawford [39] to explain the
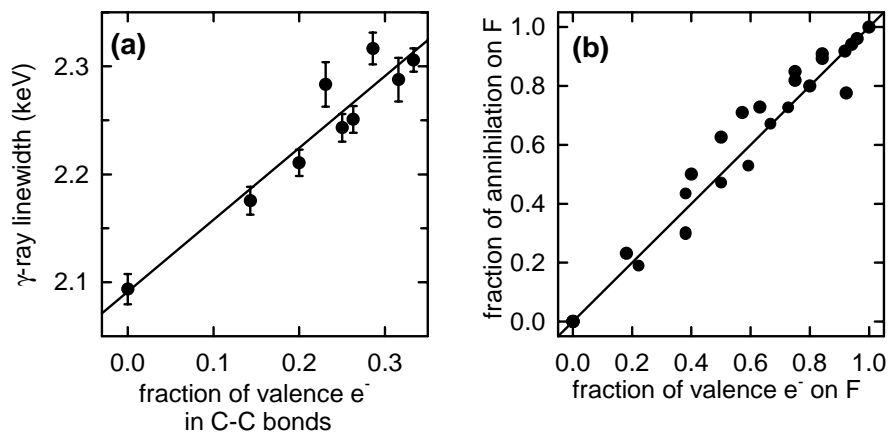

Figure 5. (a) Gamma-ray line width for alkanes (•), plotted against the fraction of valence electrons in C-C bonds, and (−) a linear fit to the data. (b) Fraction of annihilation on fluorine atoms for partially fluorinated hydrocarbons (•), plotted against the fraction of valence electrons on these atoms, and (−) the line y = x. These linear relationships provides evidence that positrons annihilate with approximately equal probability on any valence electron. (See Ref. [15] for details.)

observation of significant molecular fragmentation observed following positron annihilation at energies below the threshold for positronium formation [20, 40]. Crawford predicted that annihilation on any of the valence molecular orbitals occurs with roughly equal probability [39]. Thus if the highest lying molecular orbitals do not dominate the annihilation process, the molecular ion that is produced will frequently be left in an excited electronic state. Then the excess energy in these excited states produces the fragmentation that is observed.

The measurements of annihilation rates shown in Fig. 2 were done with a Maxwellian distribution of positrons having a positron temperature $T_p = 300$ K (i.e., 0.025 eV). To investigate $Z_{eff}(T_p)$, measurements have also been done with the positrons heated above 300 K by applying radio frequency noise to the confining electrodes [29]. The annihilation rate and positron temperature are measured as the positrons cool. The experiments thus far have been limited to T_p ≤ 0.2 eV for hydrocarbon molecules and ≤ 0.8 eV for noble gas atoms; above these temperatures, the heating produces non-Maxwellian positron velocity distributions. In the noble gas studies, the dependence of Γ on T_p is in good agreement with theoretical predictions [29].

Measurements of $Z_{eff}(T_p)$, for CH_4 and CH_3F are shown in Fig. 6 (a) [15]. A study of butane (C_4H_{10}) indicates that the temperature dependence of Z_{eff} is very similar to that shown for CH_4 [15]. These data exhibit interesting features, such as an initial slope proportional to $T_p^{-1/2}$ and a break in slope at higher temperature in CH_4 and C_4H_{10}, which have recently begun to be considered theoretically [15, 16]. This 'plateau' at higher temperatures may be due to the excitation of molecular vibrations.
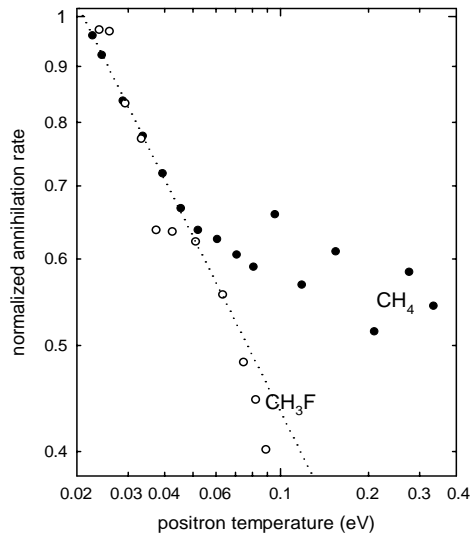

Figure 6. Dependence of annihilation rates on positron temperature: (•) methane (CH_4), and (O) fluoromethane (CH_3F). The annihilation rates are normalized to their room-temperature values. The dotted line (⋯) is a power law fit to the lower temperature data with the coefficient of –0.53.

Building upon previous work [6 12], Gribakin has proposed a comprehensive theoretical model of annihilation in molecules [16]. While many open questions remain, this theory provides a useful framework for considering the annihilation process and its dependence on molecular species. A key assumption is that the positron-hydrocarbon potential is sufficiently attractive to admit bound states. The wide variation in the values of Z_{eff} for various species is then explained in

terms of positron-molecule resonances. Values of Z_{eff}, much larger than Z but $\leq$ 10^3 are predicted to occur via either low-lying positron-molecule resonances or weakly bound states. However Gribakin concludes that larger values of Z_{eff} *cannot* be explained by such a mechanism. He predicts that values of Z_{eff} larger than 10^3 arise from the excitation of vibrationally excited quasi-bound states of the positron-molecule complex, an idea that was proposed previously to explain the values of Z_{eff} observed in large molecules such as alkanes [12]. The vibrational density of states of a molecule increases very rapidly as a function of increasing molecular size. When the positron-molecule potential is attractive, this increased density of states leads to a corresponding increase in Z_{eff}.

Qualitatively, the basis of Gribakin's model is that, when there are shallow bound states or low-lying resonances, the cross section diverges as a^{-2}, where a is the scattering length, and this leads to large values of Z_{eff}. However, for room temperature positrons, the cross section σ is limited by the finite wave number, k, of the positron to $\sigma \leq 4\pi/k^2$, which in turn limits Z_{eff} to $\sim 10^3$. In large molecules in which the positron-molecule potential is attractive, the high density of vibrational states increases greatly the probability of resonance formation, and this results in even larger values of Z_{eff}. The limit occurs when the lifetime of the resonances is comparable to the annihilation time of a positron in the presence of molecular-density electrons, which corresponds to values of $Z_{eff} \sim 10^7 - 10^8$ [15, 16].

The theoretical framework proposed by Gribakin makes a number of predictions, several of which are in qualitative agreement with experiment. The model provides a natural explanation for the qualitative differences in Z_{eff} observed for fluorocarbons and hydrocarbons (c.f., Fig. 2) [15, 16]. The positron-fluorine potential is likely to be less attractive than that between the positron and C - H bond electrons. As a result, fluorocarbon molecules are not expected to bind positrons, and hence there will be no resonant enhancement in Z_{eff}. This explains the very large differences in Z_{eff} observed for the two chemical species.

Similarly, the model appears to explain in a natural way the peaks in annihilation rate observed in partially fluorinated hydrocarbons when the molecule contains only one or two fluorine atoms. In this case, Gribakin predicts that the peaks are due to the position of the bound/virtual levels moving to zero energy as a result of changes in the degree of fluorination. This produces a divergence in the scattering length and hence a large value of Z_{eff}. The data are qualitatively in agreement with Gribakin's predictions. The model predicts that Z_{eff} is proportional to the elastic scattering cross section which, as discussed below, could possibly be tested by scattering experiments with a very cold positron beam. The model also predicts that $Z_{eff} \sim T_p^{-1/2}$ in the regime where $Z_{eff} > 10^3$ and at low values of positron temperature [16]. This scaling is observed for both methane and butane. The butane result is consistent with the theoretical prediction while, in the framework of Gribakin's model, the methane scaling appears to be due to a combination of effects [15].

10

There still remain a number of open questions. One is the observation that deuteration of hydrocarbons produces only relatively small changes in Z_{eff}, even though the C-H vibrational frequencies are changed by $\sim 2^{1/2}$ [Iwata, 2000]. If the large values of Z_{eff} are due to vibrationally excited resonances, then change in the vibrational mode frequencies might be expected to produce changes in the vibrational density of states and hence relatively large changes in Z_{eff}. The experimental results may mean that only low-frequency vibrational modes contribute to the formation of the vibrationally excited resonances.

Another puzzling question is the origin of the empirical scaling of Z_{eff} with $(E_i - E_{Ps})^{-1}$ [i.e., shown in Fig. 3] that is observed for all of the atoms and single-bonded molecules studied. While this scaling fits the data over six orders of magnitude in Z_{eff} to within in a factor ≤ 10, it remains to be seen whether it has any theoretical significance. If there were low-lying *electronic* excitations of a positron-atom or positron-molecule complex, then a resonance model might be possible without involving molecular vibrations. However, there appears to be no analogous phenomenon involving low-lying electronic excitations in electron-molecule interactions, and so the positron would have to play a fundamental role in such modes. This appears to be unlikely. A more plausible explanation is that the quantity $(E_i - E_{Ps})^{-1}$ is a measure of the attraction of the positron to the atom or molecule, and so increases in this parameter increase Z_{eff} in accord with both the Murphy *et al.* scaling and Gribakin's model.

The first challenge will be to test the general validity of models for the large values of Z_{eff}. Beyond this, there also remain a number of trends in Z_{eff} with specific chemical species. For example, modest changes in chemical structure can change Z_{eff} by factors of 3 to 10 or more (e.g., differences in ring and chain molecules, for example). Experimental tools such as those discussed in this chapter and the considerable theoretical activity evidenced elsewhere in the volume, may well provide new insights in the not too distant future into the many remaining questions concerning large annihilation rates observed in molecules.

4.   SCATTERING FROM ATOMS AND MOLECULES

The development of cold, bright trap-based positron beams has enabled new kinds of scattering experiments. In this section, we restrict the discussion to recent measurements that have been made using this technique. The principles of operation of the cold beam and the procedures for these scattering experiments, which are conducted in a magnetic field, are described in detail elsewhere [18, 19, 32, 33, 41]. After the positrons are trapped and cooled in the accumulator, the potential of the bottom of the trap is slowly raised, and the positrons are pushed over a potential barrier of height V_B, as illustrated in Fig. 7. The positrons are guided magnetically through a gas cell to a retarding potential analyzer (RPA). The parallel energy distribution of the beam can be measured using the adjustable voltage V_A when no gas is present in the cell. This technique results in positron

beams with very narrow parallel energy distributions (e.g., $\leq$ 20 meV, FWHM) over a wide range of beam energies from ~ 0.05 eV to many electron Volts. The energy spread of the positron energy perpendicular to the magnetic field is also small (i.e., ~ 25 meV).

Since the beam is formed in the presence of the magnetic field of the positron accumulator (B ~ 0.15 T), it is convenient to study scattering from atoms and molecules in a magnetic field of comparable strength. This is in contrast to more conventional methods to study scattering that use either an electrostatic beam or a very weak magnetic guide field (e.g., B ~ 0.001 T). Referring to Fig. 7, the positron beam passes through the cell containing a test gas, where the beam energy is set by the gas cell potential V_C [i.e., the positron beam energy in the cell is $e(V_B - V_C)$]. The parallel energy of the transmitted beam (i.e., composed of both scattered and unscattered particles) is then analyzed using the RPA.

The method of analysis relies on the fact that the positron orbits are strongly magnetized (i.e., particle gyroradii $\leq$ 10 μ) [18, 41]. In this case the motion of the positrons can be separated into components parallel and perpendicular to the applied magnetic field. With the exception of the short time intervals during which scattering events take place, the quantity $E_\perp/B$ is a constant, where $E_\perp$ is the energy of the positron due to the velocity components perpendicular to the field. In the language of classical mechanics and plasma physics, the quantity $E_\perp/B$ is an adiabatic invariant, which is valid in the limit that the magnetic field in the rest frame of the positron varies slowly compared to the period of the cyclotron motion of the particle [42].
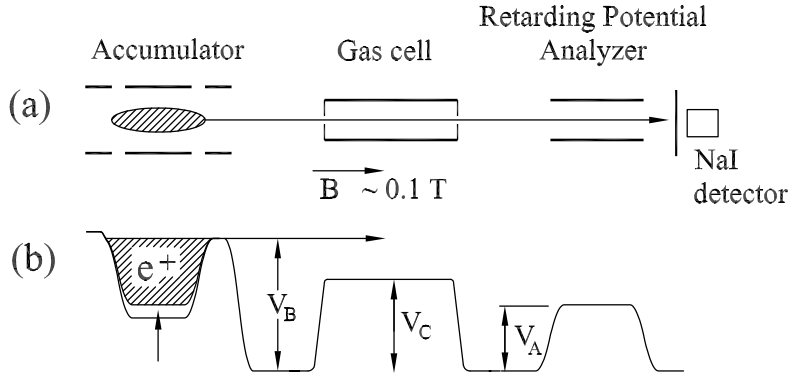

Figure 7. (a) Schematic diagram of the apparatus to form a cold positron beam and to study scattering in a magnetic field; (b) the corresponding potential profile.

It is then convenient to write the total energy of the positron as:

$$E = E_{||} + E_\perp, \tag{2}$$

where $E_{||}$ is the energy in the motion parallel to the magnetic field. Elastic and inelastic scattering in this limit are illustrated in Fig. 8 (a) for a beam with initial

12

energy E = 1.0 in the units of the figure. The beam is assumed to be "cold," so that initially $E_{||} >> E_{\perp}$. Elastic scattering converts $E_{||}$ into $E_{\perp}$ at constant *E,* resulting in a distribution of particles located around the 45° line in Fig. 8 (a), given by $E = E_{||} + E_{\perp} = 1$. Thus when no *inelastic* scattering is present, measurement of only the parallel energy of the scattered particle can be used to uniquely determine the scattering angle by the relation

$$\theta = \sin^{-1}[(E_{\perp}/E)^{1/2}]. \qquad\qquad (3)$$

A study of elastic scattering of 1 eV positrons from argon atoms using this technique is illustrated in Fig. 9, which is made possible by the fact that there is no open inelastic channel in argon at 1 eV. Figure 9 (a) shows the retarding potential curves for the unscattered and scattered beams. The normalized difference between the two curves at retarding potential V_A is the fraction of scattered particles $I(E_{||})$ with parallel energies $E_{||} \leq V_A$. The differential elastic cross section, $d\sigma/d\Omega$ is then proportional to $dI(E_{||})/d\,E_{||}$ [18, 41], and is shown in Fig. 9 (b). Since the measurement is normalized to the strength of the transmitted beam, this technique conveniently provides absolute measurement of the probability that a positron scatters in transiting the cell. This, in turn, facilitates measurement of the absolute value of the scattering cross section.

When both elastic and inelastic scattering are present, the parallel energy distributions for the two processes can overlap. This is due to the fact that elastic scattering at an angle results in a decrease in $E_{||}$, which is indistinguishable in an RPA measurement from a loss in the total energy of the positron. Thus it is not possible to distinguish the two processes. However, if the scattered beam is analyzed in a region of much lower magnetic field strength, the adiabatic invariance of $E_{\perp}/B$ results in most of the energy in $E_{\perp}$ transferred to the $E_{||}$ component. In particular, if there is a magnetic field ratio, *M*, between the magnetic field at the scattering cell and the field at the RPA, then $E_{\perp}$ is reduced by a factor of M. Using this technique, the parallel energy spreads of the elastically and inelastically scattered particles can be greatly reduced, and so the inelastic and elastic scattering can be distinguished by an RPA measurement of the parallel energy distribution. This is illustrated in Fig. 10 for the vibrational excitation of CO at an incident positron energy of 0.5 eV.

Scattering measurements using the cold beam and the analysis techniques described above began only recently [18, 19, 41], and so relatively few results are available as compared with the potential utility of the technique. We summarize the current state of experiments in three areas. To date, the technique has been used to measure differential elastic scattering when no inelastic processes are present (e.g., scattering from noble gases below the thresholds for positronium formation and electronic excitation). The technique has also been used to measure cross sections for inelastic vibrational excitation of molecules and to make a limited number of measurements of total cross sections. Low-energy differential elastic scattering cross sections have been measured in noble gases
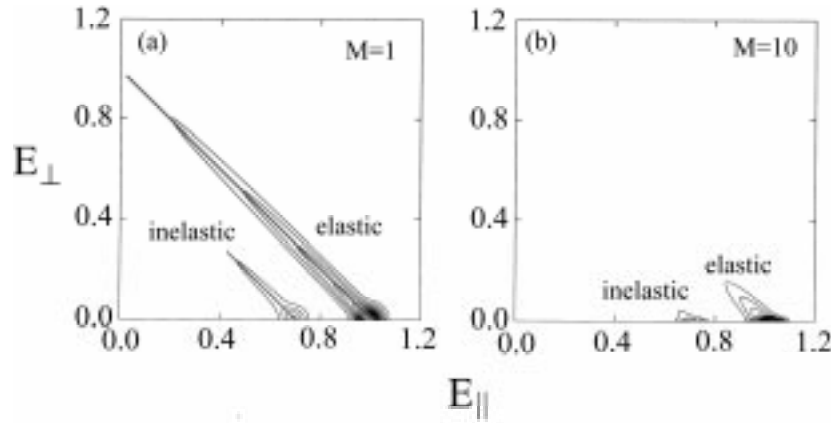
Figure 8. Simulation of the scattering of particles, with initial energy $E_{//} = 1.0 \gg E_{\perp}$, initially traveling parallel to a strong magnetic field. (a) Examples of elastic and inelastic scattering processes: for an elastic event, scattering redistributes some of $E_{//}$ into $E_{\perp}$; in the case of inelastic scattering, there is both an energy shift (~ 0.3 in this example) and also a redistribution in $E_{//}$ - $E_{\perp}$ space when the particle scatters at an angle to the field. (b) For an assumed magnetic field ratio M = 10 between the scattering cell and the RPA, the spread in $E_{\perp}$ is greatly reduced, so that an RPA measurement can distinguish elastic and inelastic scattering. (Typically M > 30 in current experiments.)
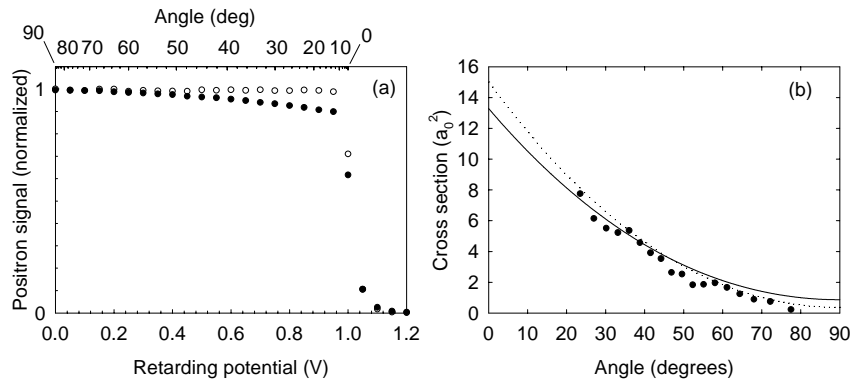

Figure 9. RPA data for positron-argon scattering at 1 eV: (a) (O) transmitted beam with no gas present, and (•) with argon in the gas cell. (b) differential elastic scattering cross section. Solid and dotted lines show the theoretical predictions of Refs. [43] and [44] respectively. Data and theory are folded about 90^0, since the experiment did not distinguish forward and back scattering. See Refs. [18] and [41] for details.

down to about 0.4 eV [18, 41]. The data are in good absolute agreement with theoretical predictions, as illustrated in Fig. 9 (b). The measurements done to date have the ambiguity that back scattering and forward scattering cannot be resolved separately. (See Ref. [41] for details.) It is possible to arrange the experiment to measure only forward-scattered particles (i.e., $\theta \leq 90^0$), but this has

14

not yet been done. In principal, the scattering measurements can be made down to energies close to the resolution of the beam (e.g., $\varepsilon \leq 50$ meV). At present, there are experimental difficulties in making measurements at positron energies ≤ 0.2 eV. These problems appear to be due to small potential differences on the gas cell electrodes (e.g., $\Delta V \leq 0.1$ V). They do not appear to be intrinsic and can likely be resolved.

Inelastic scattering cross sections can be measured if the energy separation between different processes is ~ 30 - 40 meV (i.e., greater than the parallel energy spread of the beam). Perhaps the most interesting physics results obtained thus far using the techniques described here are the first studies of the inelastic
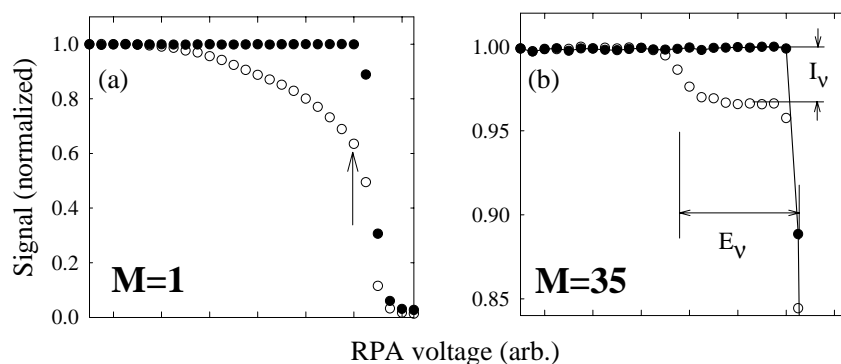

Figure 10. (a) RPA measurement for CO using a 0.5 eV positron beam and magnetic field ratio, M = 1; (b) the same measurement at M = 35. The step marked by the arrow in (b) corresponds to excitation of the v_1 mode in CO at an energy $E_v = 0.27$ eV. Note the expanded vertical scale in (b). There is excellent discrimination between elastic scattering [~ 35%, as shown in (a)], and the vibrational inelastic scattering, with relative amplitude, $I_v \sim 4\%$, as shown in (b). The point labeled by the vertical arrow in (a) includes both inelastic and elastic scattering and is therefore a measure of the total scattering cross section. (From Ref. [19].)

vibrational excitation of molecules by positrons. This is illustrated in Fig. 10 for the case of CO. Thus far CO, CO_2, H_2, CF_4 and CH_4 have also been studied [18, 19], and the list will likely grow quickly. Shown in Fig. 11 are data for H_2 and CO_2, together with available theoretical predictions. There is reasonable-to-good absolute agreement between theory and experiment for both molecules. Two modes were resolved in CO_2, with the lowest having an energy of only 0.08 eV. As can be seen in the figure, there are still discrepancies between theory and experiment for H_2, and there are gaps in the comparisons for CO_2, so that further work is warranted.

There is similar agreement between theory and experiment for CO in the range of positron energies studied to date (i.e., $0.5 \leq \varepsilon \leq 5$ eV) [19]. The data in most cases are sufficiently accurate that they might be used to guide further improvements in the calculations. At present, we are not aware of theoretical predictions for CF_4 and CH_4, but a number of groups have expressed interest in calculating cross sections for these and other molecules. The list of interesting

molecules is long and many questions remain, including understanding the qualitative differences in the behavior of positron and electron vibrational excitation cross sections for particular modes and molecules. The behavior of the cross sections at and near threshold is also of interest and is currently being studied.

The method described here also lends itself to absolute measurements of total cross sections as a function of energy, and experiments of this type have begun.
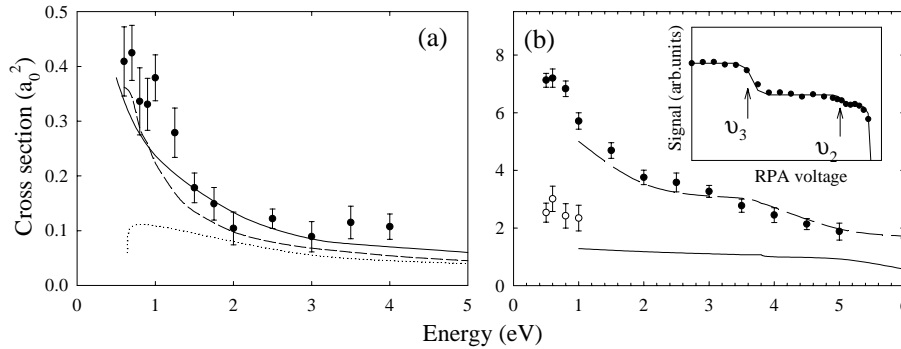

Figure 11. (a) Measurement of the cross section for excitation of the ν_1 vibrational mode of H_2 as a function of positron energy. Also shown are theoretical predictions: (-) Sur and Ghosh [45], (…) Baille and Darewych [46], and (--) Gianturco and Mukherjee [47, 48]. (b) Cross sections for the ν_2 and ν_3 modes of CO_2 at 0.08 and 0.29 eV respectively. Also shown are the theoretical predictions of Ref. [49] (See Ref. [19] for details.)

The total cross section is obtained by measuring the amplitude of the beam transmitted through the gas cell at a retarding potential just below that corresponding to the beam energy; this value will include both the elastic and inelastic scattering components. This is illustrated in Fig. 10 (a), for the case of CO, where both elastic and inelastic vibrational channels are open. In particular, the point labeled by the vertical arrow in Fig. 10 (a) includes both the inelastic and elastic scattering (except very near forward scattering). It is of interest to use the cold beam to extend to lower energies the many previous measurements for total cross sections done using other techniques [1, 10, 11].

5. A LOOK TO THE FUTURE

5.1 Positron Annihilation

One focus will be understanding the large annihilation rates, $Z_{eff} >> Z$, observed for large molecules. Doppler broadening measurements indicate that

the annihilation takes place with approximately equal probability on any valence electron. Based on the limited studies done thus far varying positron temperature, the ability to make *energy resolved* measurements of Z_{eff} appears as if it could provide new insights into the annihilation process. For example, in small molecules, we would be able to search for possible increases in annihilation rates associated with the excitation of specific vibrational modes. We are currently building an annihilation measuring apparatus that will allow such energy-resolved annihilation measurements using the cold positron beam. Estimates indicate that values $Z_{eff} \geq 10^3$ can be studied conveniently, and this sensitivity limit can likely be improved.

Annihilation on very large molecules (i.e., with low vapor pressures), atomic clusters, and dust grains is also of interest. For example the large hydrocarbon molecule, pyrene, which is an arrangement of four benzene rings, is prototypical of polycyclic aromatic ("PAH") molecules present in the interstellar medium. Based upon measurements of smaller molecules with similar structure, pyrene is expected to have values of Z_{eff} in excess of 10^7 [50]. The high annihilation rate of this molecule has potentially important implications in astrophysics. Low vapor-pressure materials are difficult to study directly in the positron accumulator, because the large values of Z_{eff} result in a precipitous loss of positrons and deterioration in trap performance. An annihilation experiment using a positron beam, such as that described in the preceding paragraph, would provide the opportunity for a sample cell located external to the positron accumulator. Such a cell could be operated at an elevated temperature and could also be configured with the required vacuum isolation between the accumulator and gas cell. This arrangement would then enable studies of many interesting low-vapor pressure materials, including very large molecules, atomic clusters and dust grains. This experiment would also be useful for studying annihilation on metal atoms, where predictions for annihilation rates have recently become available (i.e., as discussed in the chapters by Mitroy and Mella in this volume).

Another annihilation phenomenon of interest is the production of Auger electrons that is expected when positrons annihilate on inner-shell electrons (e.g., in Xe and Kr). Since they are born in the magnetic field of the positron trap, they will be confined to move along magnetic field lines; consequently they should be able to be detected relatively easily.

5.2   Scattering studies

5.2.1   Inelastic Scattering

There are many possible future directions for this research, some of which were discussed above. Inelastic cross section measurements at positron energies $\varepsilon \geq 0.2$ eV and with an energy resolution ~ 20 meV are now relatively straightforward. There are a number of interesting phenomena that can be

studied with this technique, such as vibrational excitation of molecules, as illustrated in Fig. 11. We are also beginning to study the *electronic* excitation of atoms and molecules, exploiting the high resolution available with the cold beam. This technique could also be useful to investigate sharp electronic resonances that are predicted to occur near electronic transitions in various atoms and molecules, a subject which is discussed in more detail in the chapter by Buckman.

5.2.2   Elastic Scattering

As discussed above, differential elastic cross sections can now be measured down to $\varepsilon \geq 0.4$ eV and inelastic and total cross sections can be measured down to about ≥ 0.2 eV; work to extend these measurements to lower energies is now underway. The present experiments do not distinguish forward and back scattering, but measure the cross section for both processes folded about 90^0, i.e., $\sigma_{meas} = \sigma(\theta) + \sigma(\pi - \theta)$. This limitation can potentially be overcome by insertion of an *E x B* filter in between the positron accumulator and scattering cell to remove the back-scattered particles before they are detected.

5.2.3   Total Scattering Cross Sections

Measurement of the low-energy behavior of the elastic scattering cross section, σ_{el} can, in principal, be used to study weakly bound states and resonances, which are expected to occur at energy

$$\varepsilon_0 = (1/2m)(h/2\pi a)^2, \tag{4}$$

where h is Planck's constant, a is the zero-energy scattering length, and m is the positron mass [16]. The scattering length a is positive in sign for a bound state and negative for a resonance. In the asymptotic limit in which the positron momentum, $k << 1/a$, where k is in units of wave number, the elastic scattering cross section is given by $\sigma_{el} = \pi a^2$.

Thus measurement of the total cross section provides a measurement of the magnitude of the scattering length and hence the binding energy. In this same limit, the sign of $d\sigma_{el}/d\varepsilon$ determines the sign of a, where ε is the energy of the incident positron. The existence of such bound states and resonances play a crucial role in Gribakin's model for positron annihilation in molecules for $Z_{eff} \leq 10^3$, and so low-energy scattering studies could provide a rather direct test of the model. The challenge in this experiment will be to make the measurement in a regime in which Eq. 4 is valid, which may require a *very* low energy positron beam (e.g., $ka \leq 0.1$, which corresponds to $\varepsilon \sim 1 - 10$ meV).

A related topic is the peak in Z_{eff} that is observed when one or two fluorine atoms are substituted for hydrogens in hydrocarbon molecules. Gribakin predicts that this peak in Z_{eff} is due to the divergence in the scattering length when a bound state (hydrocarbon limit) turns into a virtual state (fluorocarbon limit).

This prediction could also be checked by such a low energy scattering experiment.

These discussions of low energy scattering experiments raise the question as to the limit in energy resolution of the cold beam technique. We are currently building an apparatus to create a cryogenic [e.g., $T_p \sim 10$ K (1 meV)] positron plasma [34]. This technique uses a 5 T magnetic field and a cooled electrode structure, so that the positron plasma will come to thermal equilibrium with the walls via cyclotron radiation. In principle, this could permit the formation of a cold beam with energy resolution comparable to T_p, which would be useful, for example, in making the measurements of the scattering length described above. Such a beam could also be used to study the rotational excitation of molecules by positron impact. Nevertheless, the difficulties in making scattering measurements with such a cold beam, while still maintaining the required energy resolution, should not be minimized.

Finally, we mention another technical detail: A new technique for manipulating trapped positron plasmas has been developed that will be useful in future scattering and annihilation experiments. Recently, positron plasmas have been compressed radially using a rotating electric field (e.g., compressing a positron plasma radius of 4 mm to 0.7 mm) [35, 36]. This technique will be useful in scattering experiments in improving vacuum isolation of the gas cell, since the beam can then be passed through much smaller apertures. Similarly, it will be useful in positron beam annihilation experiments to achieve good vacuum isolation and also to keep the beam away from surrounding surfaces that would cause a background annihilation signal.

6.   CONCLUDING REMARKS

While positron atomic and molecular physics research has been conducted for decades, it is fair to say that research with low-energy positrons and high-resolution positron sources is much less mature. The advent of positron accumulators and trap-based beams offer many new opportunities. The results thus far are promising, and the corresponding response from the theoretical community is very encouraging. It is likely that, in the next decade, we will expand greatly our understanding of low-energy positron-matter interactions. This knowledge can be expected to be important in many fields of science, ranging from astrophysics and condensed matter physics, to providing the quantitative basis of an antimatter-matter chemistry, to the creation and study of stable, neutral antimatter such as antihydrogen.

References

[1]   W. E. Kauppila and T. S. Stein, J. Adv. Atomic, Mol. & Opt. Phys. **26** (1990).
[2]   P. J. Schultz and K. G. Lynn, Rev. Mod. Phys. **60**, 701-79 (1988).
[3]   N. Guessoum, R. Ramaty, and R. E. Lingenfelter, Astrophys. J. **378**, 170 (1991).
[4]   L. D. Hulett, Mat. Sci. Forum **99**, 175-78 (1995).
[5]   D. A. L. Paul and L. Saint-Pierre, Phys. Rev. Lett. **11**, 493 (1963).
[6]   P. M. Smith and D. A. L. Paul, Can. J. Phys. **48**, 2984-2990 (1970).
[7]   D. M. Schrader and R. E. Svetic, Can. J. Phys. **60**, 517 (1982).
[8]   G. R. Heyland, M. Charlton, T. C. Griffith, *et al*., Can. J. Phys. **60**, 503 (1982).
[9]   M. Charlton and G. Laricchia, J. Phys. B **23**, 1045 (1990).
[10]   O. Sueoka and A. Hamada, J. Phys. Soc. Japan **62**, 2669-74 (1993).
[11]   M. Kimura, O. Sueoka, A. Hamada, *et al*., Adv. Chem. Phys. **111**, 537 (2000).
[12]   C. M. Surko, A. Passner, M. Leventhal, *et al*., Phys. Rev. Lett. **61**, 1831-4 (1988).
[13]   T. J. Murphy and C. M. Surko, Phys. Rev. Lett. **67**, 2954-7 (1991).
[14]   K. Iwata, R. G. Greaves, T. J. Murphy, *et al*., Phys. Rev. A **51**, 473-87 (1995).
[15]   K. Iwata, G. F. Gribakin, R. G. Greaves, *et al*., Phys. Rev. A **61**, 022719-1-17 (2000).
[16]   G. F. Gribakin, Phys. Rev. A **61**, 22720-1-13 (2000).
[17]   F. A. Gianturco and T. Mukherjee, Euro. Phys. J. D **7**, 211 (1999).
[18]   S. J. Gilbert, R. G. Greaves, and C. M. Surko, Phys. Rev. Lett. **82**, 5032 (1999).
[19]   J. Sullivan, S. J. Gilbert, and C. M. Surko, Phys. Rev. Lett. **86**, 1494 (2001).
[20]   J. Xu, L. D. Hulett, Jr., T. A. Lewis, *et al*., Phys. Rev. A **47**, 1023-30 (1993).
[21]   M. Charlton and G. Laricchia, Hyperfine Inter. **76**, 97-113 (1993).
[22]   J. Eades and F. J. Hartmann, Rev. Mod. Phys. **71**, 373-419 (1999).
[23]   M. H. Holzscheiter and *et al*., Nucl. Phys. B. **56A**, 336-48 (1997).
[24]   R. G. Greaves and C. M. Surko, Phys. Plasma **4**, 1528-1543 (1997).
[25]   T. Yamazaki, E. Widmann, R. S. Hayano, *et al*., Nature **361**, 238-240 (1993).
[26]   P. Froelich, S. Jnsell, A. Saenz, *et al*., Phys. Rev. Lett. **84**, 4577 (2000).
[27]   C. M. Surko, M. Leventhal, and A. Passner, Phys. Rev. Lett. **62**, 901-4 (1989).
[28]   T. J. Murphy and C. M. Surko, Phys. Rev. A **46**, 5696-705 (1992).
[29]   C. Kurz, R. G. Greaves, and C. M. Surko, Phys. Rev. Lett. **77**, 2929-32 (1996).
[30]   S. Tang, M. D. Tinkle, R. G. Greaves, *et al*., Phys. Rev. Lett. **68**, 3793-6 (1992).
[31]   K. Iwata, R. G. Greaves, and C. M. Surko, Phys. Rev. A **55**, 3586-3604 (1997).
[32]   S. J. Gilbert, C. Kurz, R. G. Greaves, *et al*., Appl. Phys. Lett. **70**, 1944-1946 (1997).
[33]   C. Kurz, S. J. Gilbert, R. G. Greaves, *et al*., Nucl. Instrum. Methods in Phys. Res. **B143**, 188 (1998).
[34]   C. M. Surko, S. J. Gilbert, and R. G. Greaves, Non-Neutral Plasma Phys. III, edited by J. J. Bollinger, R. L. Spencer, and R. C. Davidson (American Institute of Physics, New York) , 3-12 (1999).
[35]   R. G. Greaves and C. M. Surko, Phys. Rev. Lett. **85**, 1883 (2000).
[36]   R. G. Greaves and C. M. Surko, Phys. Plasmas **in press** (2001).
[37]   P. VanReeth, J. W. Humberston, K. Iwata, *et al*., J. Phys. B **29**, L465-71 (1996).
[38]   S. Y. Chuang and B. G. Hogg, Il Nuovo Cimento **58B**, 381 (1968).
[39]   O. H. Crawford, Phys. Rev. A **49**, R3147-50 (1994).

[40]   L. D. Hulett, D. L. Donohue, J. Xu, *et al*., Chem. Phys. Lett. **216**, 236-240 (1993).

[41]   S. J. Gilbert, J. Sullivan, R. G. Greaves, *et al*., Nucl. Instrum. Methods in Phys. Res. **B171**, 81-95 (1999).

[42]   L. D. Landau and E. M. Lifshitz, Course in Theoretical Physics, Vol. 1, Mechanics, Permagon Press, New York (1959).

[43]   R. P. McEachran, A. G. Ryman, and A. D. Stauffer, J. of Phys. B **12**, 1031-31 (1979).

[44]   V. A. Dzuba, V. V. Flambaum, G. F. Gribakin, *et al*., J. Phys. B **29** (1996).

[45]   S. Sur and A. S. Ghosh, J. of Phys. B **18**, L715 (1985).

[46]   P. Baille and J. W. Darewych, J. de Phys. Lett. **35**, 243-45 (1974).

[47]   F. A. Gianturco and T. Mukherjee, J. Phys. B: At. Mol. Opt. Phys. **30**, 3567-81 (1997).

[48]   F. A. Gianturco and T. Mukherjee, Phys. Rev. A , submitted (2001).

[49]   M. Kimura, et al, Phys. Rev. Lett. **80**, 3936 (1998).

[50]   K. Iwata, R. G. Greaves, and C. M. Surko, Can. J. Phys. **51**, 407-10 (1996).